MULTIVARIATE STATISTICAL MODELLING TO CORRELATE PECVD LAYER PROPERTIES WITH PLASMA CHEMISTRY DURING SILICON NITRIDE DEPOSITION

L. Rachdi, M. Hofmann
Fraunhofer Institute for Solar Energy Systems ISE
Heidenhofstr. 2, 79110 Freiburg, Germany

ABSTRACT: Optical emission spectroscopy (OES) was performed during the deposition of SiN_x layers in an industrial-scale plasma-enhanced chemical vapor deposition (PECVD) tool. Emission spectra peaks were correlated to deposition properties: deposition rate, refractive index, and bond densities. A statistical model was built to predict layer properties for silicon nitride deposition using different process parameters. This model was used to build a multivariate linear correlation between process parameters and film properties. The accuracy of the results showed a deviation of less than 10.3% for layer thickness, 1.7% for refractive index and 35.8% for bond densities. Based on these results, we propose OES as a powerful method that can be used not only to increase the process control but also for statistical modelling. Moreover, the inversion of the multivariate correlation allows calculation of the multiple sets of process parameters for depositing silicon nitride layers with given properties.
Keywords: Plasma characterization, optical emission spectroscopy, passivation

1 INTRODUCTION

Increasing the efficiency of solar cells is an effective way to lower the overall cost of photovoltaic systems [1]. Various high-efficiency, silicon-based solar cell architectures, such as PERC [2], PERT, PERL [3], TOPCon [4], and IBC [5], are either already in an advanced stage of production or still in the research phase. Regardless of the cell architecture, deposition of dielectric layers is one of the most important process steps in solar cell manufacturing. Plasma-enhanced chemical vapor deposition (PECVD) is the most widely employed method for industrially deposited dielectric passivation layers.

Due to its extensive industrial application, optimization of the PECVD process is a key requirement towards the fabrication of efficient solar cells. However, due to the complexity of physical interactions and chemical reactions in plasma, performing trial and error has been the preferred method of plasma process optimization.

On the other hand, in-situ plasma characterization has proven useful in lab scale deposition tools [6]. In-situ plasma characterization could especially be an interesting approach to better understand the role of plasma chemistry for layer growth and to provide the possibility for real-time monitoring during PECVD depositions [7]. However, it has never been used extensively for upstream design for large scale industrial application [8].

The goal of this work is to introduce in-situ plasma characterization by means of optical emission spectroscopy (OES) and to investigate the possibility for layer characteristics prediction. It is a non-intrusive and fast method of plasma characterization, which makes it ideal for industrial use.

In this work, in-situ OES characterization of silicon nitride (SiN_x) deposition in an industrial scale microwave PECVD tool is performed. First, the plasma emission spectrum is correlated to layer characteristics such as layer thickness, refractive index, and bond densities. A statistical model based on linear regression is built to fit the in-situ data of measured plasma characteristics and ex-situ data of measured layer characteristics. In the next step, this model is evaluated to predict the characteristics of dielectric layers before performing PECVD deposition.

2 EXPERIMENTAL PROCEDURE

Dielectric films were deposited using an industrial PECVD tool (MeyerBurger MAiA). The processing chamber is schematically shown in Figure 1. Processing gases are introduced and are dissociated using microwave plasma. Magnetrons at the extremities of a quartz tube generate surface waves at a microwave frequency of 2.45 GHz. These waves induce homogenous plasma around the tube, the size of which is fitted for industrial purposes [9].

In our study, we focused on the deposition of silicon nitride layers using a single microwave plasma source. A mixture of silane (SiH_4) and ammonia (NH_3) was introduced in the processing chamber. Dissociated fragments accelerated to the surface of the silicon wafer are adsorbed and facilitates the growth of thin silicon nitride layers [10]. Excited atoms and molecules were analyzed by optical emission spectrometry (OES). An optical fiber directed in parallel to the quartz tube was installed inside the processing chamber. Afterwards, light emitted by the plasma was analyzed by the spectrometer.

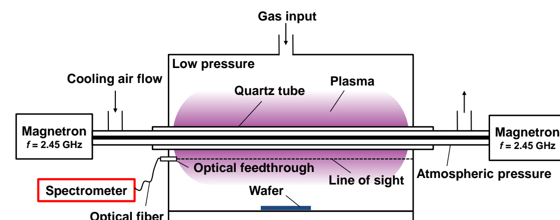

Figure 1: Schematic representation of the PECVD processing chamber with the OES. The wafer movement direction is perpendicular to the plane of the representation.

An emission spectrum was obtained during the deposition of silicon nitride layers (Figure 2). Silane and ammonia were introduced with respective gas fluxes of 200 sccm and 600 sccm. The pressure inside the chamber is 0.25 mbar and the plasma is ignited at a peak power of 3800 W. Hereafter, these conditions will be referred to as the reference conditions.

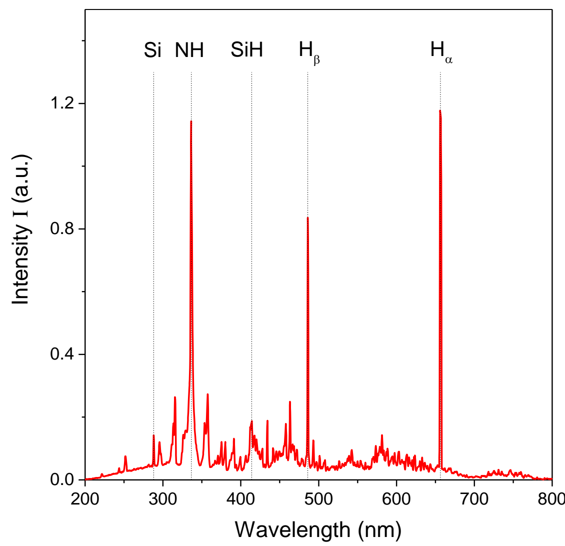

Figure 2: Typical optical emission spectrum of plasma with a mixture of silane and ammonia during PECVD deposition of SiN_x and identified main peaks.

3 METHODOLOGY

In the next step, the gas ratio of ammonia and silane was varied. The structural composition and optical properties of the deposited layers were characterized. Ellipsometry measurements fitted by a Tauc Lorenz model [11] enabled us to obtain layer thickness and refractive index at the wavelength of 630 nm. Fourier-transform infrared spectroscopy (FTIR) measurements allowed us to calculate Si-H and N-H bond densities by multiplying the Si-H (2180 nm) and N-H (3330 nm) peak areas [12] by their respective proportionality coefficients obtained from literature [13].

Optical emission peak intensities I were used to calculate emission ratios. In Figure 3, the ratio I_{Si}/I_{NH} and the refractive index are plotted together as functions of increasing the gas ratio of NH_3 to SiH_4 (Φ_{NH_3}/Φ_{SiH_4}).

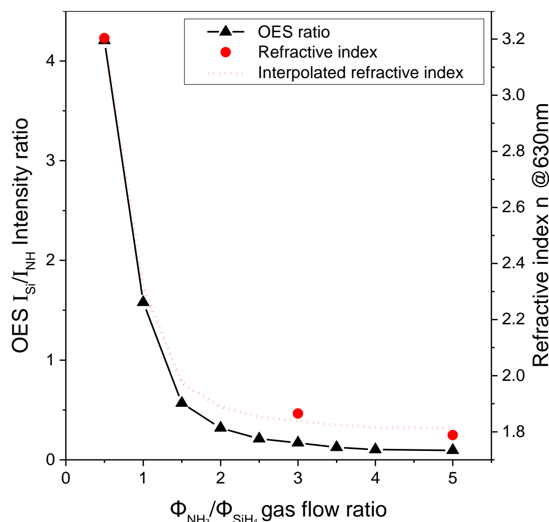

Figure 3: Correlation between I_{Si}/I_{NH} OES intensity ratio and the refractive index n, as function of gas ratio.

We can see that the OES ratio decreases with an increasing gas flow ratio. This is due to the fact that the amount of silicon-based excited species in the plasma is inversely proportional to the gas flow ratio (Φ_{NH_3}/Φ_{SiH_4}). Increasing the gas flow ratio will increase the emission intensity from NH (336 nm) and decreases that from Si (288 nm). Correspondingly, the ratio between these species I_{Si}/I_{NH} will therefore decrease.

We can also see that the refractive index of deposited silicon nitride layers decreases along with the gas flow ratio. This can be attributed to the fact that silicon-rich dielectric layers exhibit a higher refractive index than nitrogen-rich layers [14]. Increasing the gas flow ratio allows us to obtain more nitrogen rich layers, thus lowering the refractive index.

By plotting the refractive index and the OES ratio together (see Figure 3), we can see that the two curves follow the same trend. The coefficient of determination (R^2) of these two curves is found to be greater than 99%.

In Figure 3, we also can notice there are more OES experimental data points than those for the refractive index. This is because OES measurements are very fast and can be taken almost instantly, hence allowing for the collection of a large number of data points. Considering both that layer properties can be correlated to the OES signal and that it is possible to collect a large number of OES measurement data in a short time, we can interpolate the refractive index using the linear equation obtained when calculating R^2 (dashed lines in Figure 3). This method of interpolation can be generalized to the other layer characteristics and for different processing parameters. In the following section, results will be presented on refractive index, thickness, Si-H and N-H bond densities after varying pressure, power and the flows of both gases.

4 PREDICTION MODEL

In the previous paragraph, we correlated the OES intensity ratio I_{Si}/I_{NH} to the refractive index while varying the gas flow ratio between ammonia and silane. For thickness and bond densities, another set of OES intensity ratios has been calculated by fitting, using the same method described before.

A selection of results for layer interpolations is presented in Figure 4 and 5.

The interpolation of layer properties was performed by varying one processing parameter at a time (power, pressure, gas flow ratio and total gas flow), and by keeping the rest of the parameters constant at the values corresponding to the reference process. The big red dots in Figure 4 and 5 represent the training data set. This set contains experimental data from OES measurements and layer characterization. The small black dots are the predicted data calculated from the training set.

The accuracy of the interpolation when compared with a prediction set made of 6 experimental conditions (Table I) is presented in Table II.

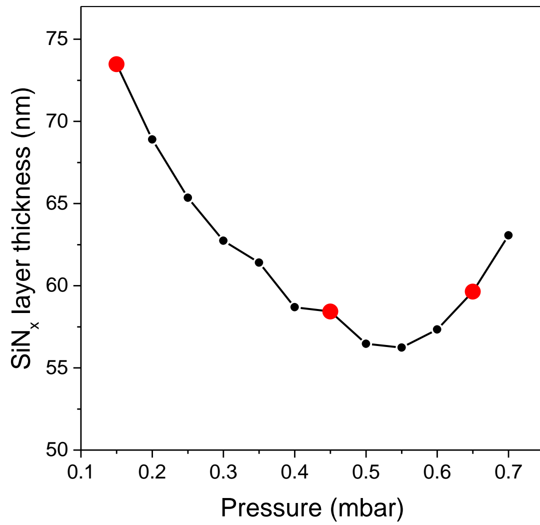

Figure 4: SiN$_x$ layer thickness interpolation with pressure variation at a fixed carrier speed of 60 cm min^{-1}.

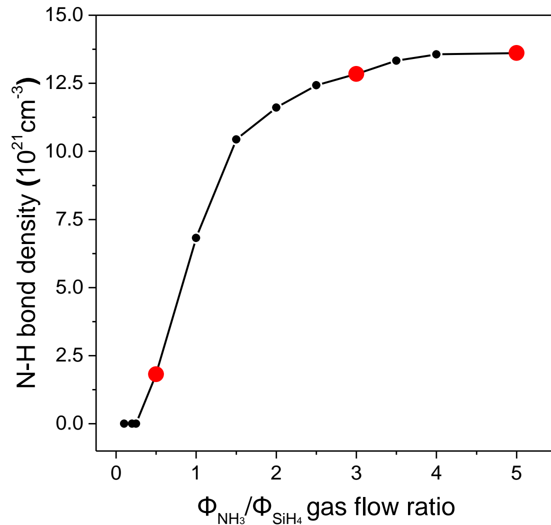

Figure 5: Change in N-H bond density in the SiN$_x$ layer with varying gas flow ratio. The big red dots are experimentally measured data points, whereas small black dots represent predicted data.

Table I: Experimental conditions for the prediction set.

Condition	Power (W)	Pressure (mbar)	Total flow (sccm)
1	2000	0.25	800
2	3000	0.25	800
3	3800	0.20	800
4	3800	0.30	800
5	3800	0.25	300
6	3800	0.25	600

Experimental values presented in Table II represent average and their respective standard deviation from a set of two samples per condition. Table II shows good agreement between the experiment and the interpolation with a maximum deviation of 10.3% for the thickness and 1.7% for the refractive index.

Table II: Comparison of the experimental set results with the predicted layer properties: layer thickness, refractive index, Si-H bond density, and N-H bond density.

Thickness (nm)			
Condition	Experimental	Prediction	Deviation
1	62.0 ± 0.2	59.3	4.3%
2	70.1 ± 0.3	72.4	-3.2%
3	76.8 ± 0.2	68.9	10.3%
4	60.2 ± 0.1	58.7	2.5%
5	40.3 ± 0.2	42.3	-5.0%
6	61.9 ± 0.1	57.5	7.2%

Refractive index n @630nm			
Condition	Experimental	Prediction	Deviation
1	2.02 ± 0.00	2.01	0.6%
2	2.00 ± 0.00	1.98	1.0%
3	1.96 ± 0.00	1.96	-0.2%
4	2.14 ± 0.00	2.11	1.7%
5	1.89 ± 0.00	1.87	0.8%
6	1.96 ± 0.00	1.94	1.1%

Si-H bond density (10^{21} cm^{-3})			
Condition	Experimental	Prediction	Deviation
1	5.5 ± 0.6	5.6	-1.6%
2	4.3 ± 0.6	3.8	13.3%
3	4.0 ± 0.5	3.9	2.6%
4	8.6 ± 0.0	7.1	18.2%
5	0 ± 0	9.1	∞
6	3.6 ± 0.4	2.3	35.8%

N-H bond density (10^{21} cm^{-3})			
Condition	Experimental	Prediction	Deviation
1	5.1 ± 0.0	5.1	1.9%
2	5.4 ± 0.2	4.6	14.3%
3	7.3 ± 0.3	5.8	19.5%
4	2.7 ± 0.1	2.6	3.7%
5	11 ± 0.5	9.2	15.2%
6	5.7 ± 0.4	7.2	-26.8%

The FTIR measurements are less accurate with a maximum error of 35.8% for the Si-H bond density calculation. This could result from a high experimental standard deviation during FTIR measurements in comparison to ellipsometry. This increased experimental variation can strongly affect the sensitivity and the fitting of the predictive model. The infinite error for Si-H bond density at a total gas flow of 300 sccm is due to the absence of a Si-H peak in the FTIR spectra due to very small SiH_4 flow. In general we can assume that for all measurements, the experimental data and the calculated results follow the same trend.

5 INVERSION MODEL

In the previous section, we proposed a correlation between layer properties and plasma optical emission data when varying one processing parameter and keeping others constant. The composition of these linear equations enables us to obtain a general equation to predict layer properties when all the parameters are varied. This multilinear correlation matrix can then be inverted to predict the processing parameters that give a set of desired layer properties.

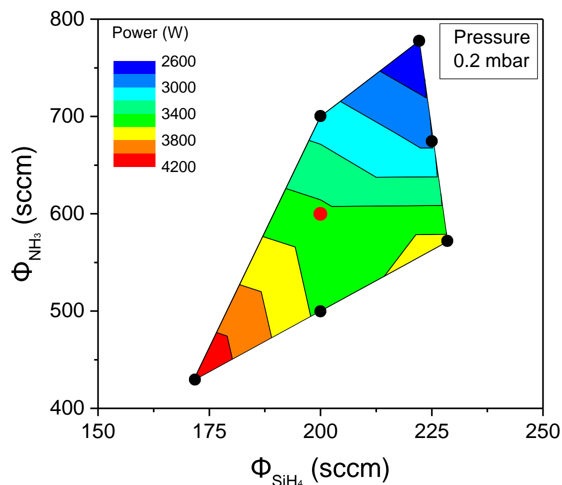

Figure 6: Contour plot of the different processing parameters (SiH_4 flow, NH_3 flow, and microwave power) predicted to give the same layer properties at a fixed pressure of 0.2 mbar. The black dots represent the discrete calculated points and the red point the reference conditions.

To obtain an exemplary set of desired layer properties (70 nm for thickness, 1.98 for refractive index, 4.10^{21} cm^3 for Si-H bond density and 7.10^{21} cm^3 for N-H bond density), we predicted a set of processing parameters, represented in Figure 6, at a fixed pressure of 0.2 mbar. This set of parameters is calculated within a degree of tolerance for every parameter. In the case shown in Figure 6, the degrees of tolerance are as follows: 10% for thickness, 2% for refractive index, 40% for Si-H and 25% for N-H bond density. The degrees of tolerance were chosen based on the importance of each layer characteristic, but also due to the accuracy of the experimental measurements. We can see that with certain conditions, the processing parameters can be optimized by reducing the amount of injected gases in comparison with the reference conditions (red dot in Figure 6). Layer characteristic results deposited with these predicted conditions and further applications of the model will be presented in a future paper.

6 CONCLUSION

In this paper, we investigated the potential of optical emission spectroscopy for PECVD process result prediction. Being a very fast and non-intrusive characterization technique, OES spectra can be used as an addition to a more typical way to model an industrial process, i.e. by directly correlating processing parameters to resulting layer characteristics. The results of the OES statistical model showed promising accuracy: less than 10.3% deviation for layer thickness, 1.7% for refractive index and 35.8% for bond densities. The inversion of the same model allowed the prediction of different process parameter sets all leading to the same layer properties.

7 ACKNOWLEDGMENTS

The authors would like to thank the German federal ministry for economic affairs and energy for the financial support of this work under the project NextStep with the contract number 0324171B.

8 REFERENCES

[1] International Technology Roadmap for Photovoltaic ITRPV, (2019).
[2] M. A. Green, "The Passivated Emitter and Rear Cell (PERC): From conception to mass production," Solar Energy Materials and Solar Cells 143, 190–197 (2015).
[3] M. A. Green, "Forty years of photovoltaic research at UNSW," Journal and Proceedings of the Royal Society of New South Wales 148, 2–14 (2015).
[4] S. W. Glunz, F. Feldmann, A. Richter, M. Bivour, C. Reichel, H. Steinkemper, J. Benick, and M. Hermle, "The Irresistible Charm of a Simple Current Flow Pattern – 25% with a Solar Cell Featuring a Full-Area Back Contact," 31st EUPVSEC 2015, 259-263 (2015).
[5] P. J. Cousins, D. D. Smith, H.-C. Luan, J. Manning, T. D. Dennis, A. Waldhauer, K. E. Wilson, G. Harley, and W. P. Mulligan, "Generation 3: Improved performance at lower cost," 35th IEEE Photovoltaic Specialists Conference, 275–278 (2010).
[6] U. Fantz, "Spectroscopic diagnostics and modelling of silane microwave plasmas," Jpn. J. Appl. Phys. 40 (6), 1035–1056 (1998).
[7] A. A. Howling, B. Strahm, P. Colsters, L. Sansonnens, and C. Hollenstein, "Fast equilibration of silane/hydrogen plasmas in large area RF capacitive reactors monitored by optical emission spectroscopy," Plasma Sources Sci. Technol. 16 (4), 679–696 (2007).
[8] M. Hofmann, M. Jäcklein, P. Saint-Cast, D. Wagenmann, B. Cord, T. Dippell, M. Dörr, T. Schütte, and M. Siemers, "Plasma Process Analysis of ICP-PECVD of AlO_x Layers for c-Si Surface Passivation," 32nd EUPVSEC 2016, 345-349 (2016).
[9] W. Petasch, E. Räuchle, H. Muegge, and K. Muegge, "Duo-Plasmaline — a linearly extended homogeneous low pressure plasma source," Surface and Coatings Technology 93 (1), 112–118 (1997).
[10] D. L. Smith, "Plasma Deposition of SiN_xH_y : Process Chemistry vs Film Properties," MRS Proc. 165 (1989).
[11] G.E Jellison, F.A Modine, "Parameterization of the optical functions of amorphous materials in the interband region," Appl. Phys. Lett. 69 (3), 371–373 (1996).
[12] F. Demichelis, F. Giorgis, and C. F. Pirri, "Compositional and structural analysis of hydrogenated amorphous silicon—nitrogen alloys prepared by plasma-enhanced chemical vapour deposition," Philosophical Magazine B 74 (2), 155–168 (1996).
[13] W. A. Lanford and M. J. Rand, "The hydrogen content of plasma-deposited silicon nitride," J. Appl. Phys. 49 (4), 2473 (1978).
[14] W. Soppe, H. Rieffe, and A. Weeber, "Bulk and surface passivation of silicon solar cells accomplished by silicon nitride deposited on industrial scale by microwave PECVD," Prog. Photovolt: Res. Appl. 13 (7), 551–569 (2005).